Effects of Cl_2-Based Inductively Coupled Plasma Etching of AlGaN on Interface Properties of Al_2O_3/AlGaN/GaN Heterostructures

Zenji Yatabe,[1,*] Yujin Hori,[1] Sungsik Kim,[1] and Tamotsu Hashizume[1,2]

[1]*Graduate School of Information and Science Technology and Research Center for Integrated Quantum Electronics (RCIQE), Hokkaido University, Sapporo 060-8628, Japan*

[2]*Japan Science and Technology Agency (JST), CREST, Tokyo 102-0075, Japan*

The effects of the inductively coupled plasma (ICP) etching of AlGaN on the interface properties of the Al_2O_3/AlGaN/GaN structures prepared by atomic layer deposition were investigated. It was found from the photoassisted *C*-*V* results that the ICP etching of the AlGaN surface significantly increased the interface state density up to 8 × 10^{12} $cm^{-2}eV^{-1}$ at the Al_2O_3/AlGaN interface. The transmission electron microscopy and X-ray photoelectron spectroscopy analyses indicated that the monolayer-level roughness, disorder of the chemical bonds at the AlGaN surface caused poor *C*-*V* characteristics due to high-density interface states at the Al_2O_3/ICP-etched AGaN interface.

[*]E-mail address mail: zenji.yatabe@rciqe.hokudai.ac.jp

AlGaN/GaN-based high-electron-mobility transistors (HEMTs) are promising for high-power switching devices, owing to a high blocking voltage and a low on-state resistance.[1-8] To realize a normally-off operation, a combination of recessed and insulated gates is often used in AlGaN/GaN HEMTs. Since the interface quality markedly affects the transistor performance, the critical processes for fabricating such devices are plasma-assisted dry etching to form the recessed gate region and the subsequent formation of an insulator-semiconductor interface. It is known that plasma-assisted etching degrades the electrical and optical properties of GaN and AlGaN surfaces.[9-12] Tang *et al.*[13] examined the SiO_2/n-GaN-based capacitors and field-effect transistors (FETs) fabricated on the GaN surfaces etched by a Cl_2-based inductively coupled plasma (ICP). They showed that ICP etching increased the interface state density and degraded the field-effect mobility of the FET channel.

Aluminum oxide (Al_2O_3) is one of the attractive insulators for a gate structure applicable to FETs and HEMTs because of its high permittivity (8-10), bandgap (7-9 eV) and breakdown field (> 10 MV/cm) values.[14,15] To obtain stable and reliable recessed oxide gate structures in AlGaN/GaN HEMTs, a low electronic state density at the Al_2O_3/AlGaN interface is absolutely required. However, no work has been reported regarding the characterization of the Al_2O_3/AGaN/GaN structures with the ICP etching of the AlGaN surface. In this letter, we thus report the effects of the Cl_2-based ICP etching of AlGaN on the interface properties of the Al_2O_3/AlGaN/GaN structures prepared by atomic layer deposition (ALD), focusing on the interface state density distribution evaluated by a photoassisted capacitance-voltage (*C-V)* technique.

The undoped $Al_{0.2}Ga_{0.8}N$/undoped GaN heterostructure grown on a sapphire substrate by metal organic chemical vapor deposition was used in this work (provided by NTT-AT), as shown in Fig. 1. The sheet resistance and mobility of the AlGaN/GaN heterostructure were 500

Ω/sq. and 1750 cm^2/Vs, respectively. The AlGaN surface was etched at RT by the ICP etching process using a Cl_2/BCl_3 gas mixture (25/5 sccm). The ICP and bias powers were 300 and 5 W, respectively. The etching depth was 7 nm at an etching rate of 10 nm/min. Following the ICP etching process, we deposited a 10-nm-thick SiN film as a surface protection layer by electron-cyclotron resonance chemical vapor deposition, in order to avoid damage to the AlGaN surface during ohmic annealing.[16)] As an ohmic electrode, a ring-shaped Ti/Al/Ti/Au (20/50/20/100 nm) multilayer structure was deposited on the AlGaN surface, followed by annealing at 800 ºC for 1 min in N_2 ambient. After the ohmic electrode process, the SiN layer was removed in a buffered HF solution. An Al_2O_3 film with a nominal thickness of 20 nm was then deposited on the AlGaN surface using an ALD system (SUGA-SAL100H) at 350 ºC for 170 cycles. In the ALD process, water vapor and trimethylaluminium were introduced into an ALD reactor in alternate pulse forms. The deposition rate of Al_2O_3 was 0.11 nm/cycle. Finally, a circular Ni/Au (20/50 nm) gate electrode was deposited on the Al_2O_3 layer.

The cross-sectional transmission electron microscopy (TEM) images of the Al_2O_3/AlGaN/AlGaN structures are shown in Fig. 2. As shown in Fig. 2(a), the thickness of the AlGaN layer decreased to 27 nm for the ICP-etched sample, corresponding to the ICP etching depth of 7 nm. Figure 2(b) shows the high-magnification images of the Al_2O_3/AlGaN interfaces with and without the ICP etching of AlGaN. The unetched sample showed a flat Al_2O_3/AlGaN interface, indicating the low-energy and layer-by-layer characteristics of the ALD process. On the other hand, ICP etching resulted in the slight roughening of the interface, creating monolayer-level steps at the AlGaN surface.

To characterize the Al_2O_3/AlGaN interface properties, we firstly performed a conventional *C-V* measurement using an HP4192 impedance analyzer at a measurement frequency of 1 MHz at RT. Figure 3 shows the typical *C-V* characteristics of the

Al_2O_3/AlGaN/GaN structures with and without the ICP etching of AlGaN. Both samples showed *C-V* curves with two steps, peculiar to the MOS sample fabricated on the heterostructure including a two-dimensional electron gas (2DEG).[17)] The constant capacitance at the forward bias corresponds to the Al_2O_3 oxide capacitance (C_{Al2O3}), whereas that at the reverse bias is determined by the total capacitance consisting of Al_2O_3 and AlGaN layers (C_{TOTAL}). At the deep reverse bias, the capacitance steeply decreases to nearly zero, indicating the 2DEG depletion at the AlGaN/GaN interface.[17)]

For the sample with ICP etching, we observed the shallower threshold voltage (V_{TH}) corresponding to 2DEG depletion. The increase in C_{TOTAL} (ΔC_{TOTAL}) is accurately equivalent to the etching depth of AlGaN (7 nm). However, the ICP-etched sample showed the gentle slope of the *C-V* curve and a high on-set voltage at the forward bias. At the forward bias, the acceptor-type interface states near the conduction band minimum can trap electrons and produce negative charges. Such an ionization of acceptor-type states screens the gate electric field, impeding the potential modulation of the AlGaN surface.[17)] This indicates the higher state densities at the Al_2O_3/AlGaN interface in the sample with ICP etching. It is likely that the high-density interface states also affect the V_{TH} behavior. The V_{TH} difference (ΔV_{TH}) between the samples with and without the ICP etching was 4.1 V, as shown Fig. 3. Using the band offsets between Al_2O_3/AlGaN and AlGaN/GaN interfaces, the 2DEG density n_s and C_{TOTAL}, we simply estimated ΔV_{TH}. *C-V* analysis using the Schottky contacts indicated that n_s decreased from 9.0×10^{12} to 7.0×10^{12} cm^{-2} after the ICP etching. As a result, ΔV_{TH} was calculated to be 3.0 V, smaller than the experimental value. For the ICP-etched sample, it is expected that the high-density negative charges due to acceptor-type states shift the V_{TH} toward the positive voltage direction, resulting in a discrepancy between the experimental and the calculated ΔV_{TH} values.

On the other hand, we observed similar *C-V* slopes at the step in the reverse bias region for both samples. In this bias region, the Fermi level is located far below the valence band maximum of AlGaN at the Al_2O_3/AlGaN interface, indicating that the electron occupation probability of interface states is no longer a function of the gate voltage.[17,18] In addition, the electrons captured at deep interface states remain almost unchanged at RT even when a large negative bias is applied to the gate electrode, because the relatively deeper states have an extremely large time constant for electron emission to the conduction band.[17] These lead to the fact that interface states act as "fixed and frozen" charges, and it is very difficult to detect interface states by a standard *C-V* measurement at RT.

To overcome this difficulty, photoassisted *C-V* measurements were performed to evaluate near-midgap interface states.[17] First, we swept the gate voltage from 0 to -11.5 V under a dark condition. Then, the gate voltage was kept at -11.5 V and the monochromatic light (MAX-302, ASAHI Spectra) with a photon energy ($h\nu$) less than the bandgap of AlGaN was illuminated to the sample surface for 120 s. Consequently, we observed the photoassisted electron emission from the interface states with the energy range corresponding to the photon energy range. After the illumination, we restarted the *C-V* sweeping toward 0 V under a dark condition. Figure 4 shows the typical photoassisted *C-V* results. When the sample surface was illuminated with a higher photon energy, a larger amount of photoassisted electron emission causes larger V_{TH} shifts in *C-V* curves. The accurately parallel *C-V* shift toward the negative direction indicates that the interface states at Al_2O_3/AlGaN act as fixed charges in this bias range. The V_{TH} difference (ΔV_{TH}) between two photon energies corresponds to the interface charge difference (ΔQ_{it}) in the energy range of E_c - $h\nu_1$ to E_c - $h\nu_2$. In the ICP-etched sample shown in Fig. 4, we observed a larger *C-V* shift (ΔV_{TH}) between two photon energies ($h\nu$ = 1.4 and 2.0 eV) than in the sample without ICP etching, indicating a higher state density at the Al_2O_3/ICP-etched AlGaN interface.

To estimate the interface state density distribution D_{it} from the photoassisted *C*-*V* results, we use the following equation:

$$D_{it} = \left(E = E_{AVG}\right) = \frac{C_{TOTAL}\Delta V_{TH}}{q\Delta h\nu}, \qquad (1)$$

where C_{TOTAL} is the series capacitance of Al_2O_3 and AlGaN, $\Delta h\nu$ is the difference between two photon energies (= $h\nu_2$ - $h\nu_1$) and E_{AVG} is the average interface state energy (= $h\nu_1 + \Delta h\nu/2$). Figure 5 shows the state density distributions at the Al_2O_3/AlGaN interfaces determined by photoassisted *C*-*V* measurement. The MOS sample without the ICP etching of AlGaN showed an interface state density of 1×10^{12} $cm^{-2}eV^{-1}$ or less near the midgap. On the other hand, high densities ranging from 3 to 8×10^{12} $cm^{-2}eV^{-1}$ were obtained at the Al_2O_3/ICP-etched AlGaN interface.

From TEM observations (Fig. 2), it was found that the ICP process introduced a monolayer-level crystalline roughness to the AlGaN surface. As a result, lattice disorder and/or a high density of dangling bonds near step edges remained at the AlGaN surface, leading to the generation of high-density electronic states with a continuous energy distribution. In fact, the TEM results showed that the number of the monolayer-level steps per unit area was approximately 5×10^{12} cm^{-2}. This value is in the same order of magnitude as the interface state densities of the ICP-etched sample shown in Fig. 5. To further investigate the degradation of the interface properties at the Al_2O_3/ICP-etched AlGaN interface, we carried out X-ray photoelectron spectroscopy (XPS) analysis on the etched AlGaN surface (not shown here). In the Ga3d spectra, the peak energy position was almost the same before and after the ICP etching. However, the full width at half maximum of the Ga3d peak slightly increased from 1.15 eV for the unetched surface to 1.21 eV for the ICP-etched one, indicating a slight disorder of chemical bonds at the AlGaN surface. There is a possibility that such chemical disorder is related to the monolayer-level steps observed in the TEM image. In addition, the XPS analysis clearly showed the decrease in the N1s peak intensity of the ICP-etched AlGaN surface. During ICP etching using the Cl_2/BCl gas mixture, active Cl^* and Cl_3 species react with the AlGaN surfaces to form volatile products, such as $GaCl_3$ and $AlCl_3$.[19,20] These dominants reaction and the subsequent formation of N_2 result in the successful etching of the AlGaN surface. However, there can be additional chemical reactions. For instance, a highly volatile NCl_3 can be produced by a reaction between the Cl-based radical and N atoms, causing a preferential loss of N atoms at the AlGaN surface.[21] Simultaneously, it seems that the complicated etching reactions with a high plasma energy introduce various kinds of defect complexes into the AlGaN surface. In fact, Fang *et al*.[22] reported that several kinds of deep levels originating from the nitrogen-vacancy (V_N)-related defect complexes were increased at the GaN surface after the Cl_2-based ICP etching. It is thus likely that ICP etching caused the monolayer-level interface roughness, disorder of the chemical bonds and formation of various types of defect complexes including V_N at the AlGaN surface, leading to poor *C-V* characteristics due to high-density interface states at the Al_2O_3/GaN interface.

In summary, we have investigated the effects of the Cl_2-based ICP etching of AlGaN on the interface properties of the Al_2O_3/AlGaN/GaN structures prepared by ALD. The *C-V* analysis at RT showed a two-step behavior, peculiar to a heterostructure MOS sample. For the sample with the ICP etching of AlGaN, the stretch-out of the *C-V* curve and the increase in on-set voltage were observed in the forward bias region, indicating high-density electronic states at the Al_2O_3/ICP-etched AlGaN interface. The photoassisted *C-V* result showed that the ICP etching of the AlGaN surface significantly increased the interface state density up to 8×10^{12} $cm^{-2}eV^{-1}$ at the Al_2O_3/AlGaN interface. The TEM and XPS analyses indicated that the monolayer-level interface roughness, disorder of the chemical bonds and various types of defect complexes including V_N at the AlGaN surface caused poor *C*-*V* characteristics due to high-density interface states at the Al_2O_3/ICP-etched AGaN interface.

References

1) H. Kambayashi, Y. Satoh, S. Ootomo, T. Kokawa, T. Nomura, S. Kato, and T. P. Chow: Solid-State Electron. **54** (2010) 660.
2) M. Kanamura, T. Ohki, T. Kikkawa, K. Imanishi, T. Imada, A. Yamada, and N. Hara: IEEE Electron Device Lett. **31** (2010) 189.
3) H. Hahn, G. Lukens, N. Ketteniss, H. Kalisch, and A. Vescan: Appl. Phys. Express **4** (2011) 114102.
4) R. Chu, A. Corrion, M. Chen, R. Li, D. Wong, D. Zehnder, B. Hughes, and K. Boutros: IEEE Electron Device Lett. **32** (2011) 632.
5) A. Nakajima, Y. Sumida, M. H. Dhyani, H. Kawai, and E. M. S. Narayanan: IEEE Electron Device Lett. **32** (2011) 542.
6) N. Otsuka, S. Nagai, H. Ishida, Y. Uemoto, T. Ueda, T. Tanaka, and D. Ueda: ECS Trans. **41** (2011) 51.
7) D. Shibata, K. Kaibara, T. Murata, Y. Yamada, T. Morita, Y. Anda, M. Ishida, H. Ishida, T. Ueda, T. Tanaka, and D. Ueda: IEDM Tech. Dig. (2011) 26.2.1.
8) M. Van Hove, S. Boulay, S. R. Bahl, S. Stoffels, X. Kang, D. Wellekens, K. Geens, A. Delabie, and S. Decoutere: IEEE Electron Device Lett. **33** (2012) 667.
9) J. Kuzmik, P. Javorka, M. Marso, and P. Kordos: Semicond. Sci. Technol. **17** (2002) L76.
10) K-J. Choi, H.-W. Jang, and J.-L. Lee: Appl. Phys. Lett. **82** (2003) 1233.
11) Z. Mouffak, A. Bensaoula, and L. Trombetta: J. Appl. Phys. **95** (2004) 727.
12) C. Cheng and J. Si: Physica B **406** (2011) 3098.
13) K. Tang, W. Huang, and T. P. Chow: J. Electron. Mater. **38** (2009) 523.
14) T. Hashizume, S. Ootomo, and H. Hasegawa: Appl. Phys. Lett. **83** (2003) 2952.
15) T. Hashizume, S. Ootomo, T. Inagaki, and H. Hasegawa: J. Vac. Sci. Technol. B **21** (2003) 1828.
16) Y. Hori, C. Mizue, and T. Hashizume: Jpn. J. Appl. Phys. **49** (2010) 080201.
17) C. Mizue, Y. Hori, M. Miczek, and T. Hashizume: Jpn. J. Appl. Phys. **50** (2011) 021001.
18) M. Miczek, C. Mizue, T. Hashizume, and B. Adamowicz: J. Appl. Phys. **103** (2008) 104510.
19) J.-M. Lee, K.-M. Chang, I.-H. Lee, and S.-J. Park: J. Electrochem. Soc. **147** (2000) 1859.
20) M. Minami, S. Tomiya, K. Ishikawa, R. Matsumoto, S. Chen, M. Fukasawa, F. Uesawa, M. Sekine, M. Hori, and T. Tatsumi: Jpn. J. Appl. Phys. **50** (2011) 08JE03.
21) T. Hashizume and H. Hasegawa: Appl. Surf. Sci. **234** (2004) 387.
22) Z.-Q. Fang, D. C. Look, X.-L. Wang, J. Han, F. A. Khan, and I. Adesida: Appl. Phys. Lett. **82** (2003) 1562.

Figure captions

Fig. 1 Schematic illustration of $Al_2O_3/Al_{0.2}Ga_{0.8}N/GaN$ MOS structure.

Fig. 2 TEM images with (a) low and (b) high resolutions for $Al_2O_3/Al_{0.2}Ga_{0.8}N/GaN$ structures with and without ICP etching.

Fig. 3 *C*-*V* characteristics of $Al_2O_3/Al_{0.2}Ga_{0.8}N/GaN$ structures with and without ICP etching measured at RT.

Fig. 4 Typical photoassisted *C*-*V* characteristics of $Al_2O_3/Al_{0.2}Ga_{0.8}N/GaN$ structures with and without ICP etching.

Fig. 5 Interface state density distributions estimated from photoassisted *C*-*V* shifts as a function of bandgap energy at $Al_2O_3/Al_{0.2}Ga_{0.8}N$ interfaces with and without ICP etching.

Figure 1

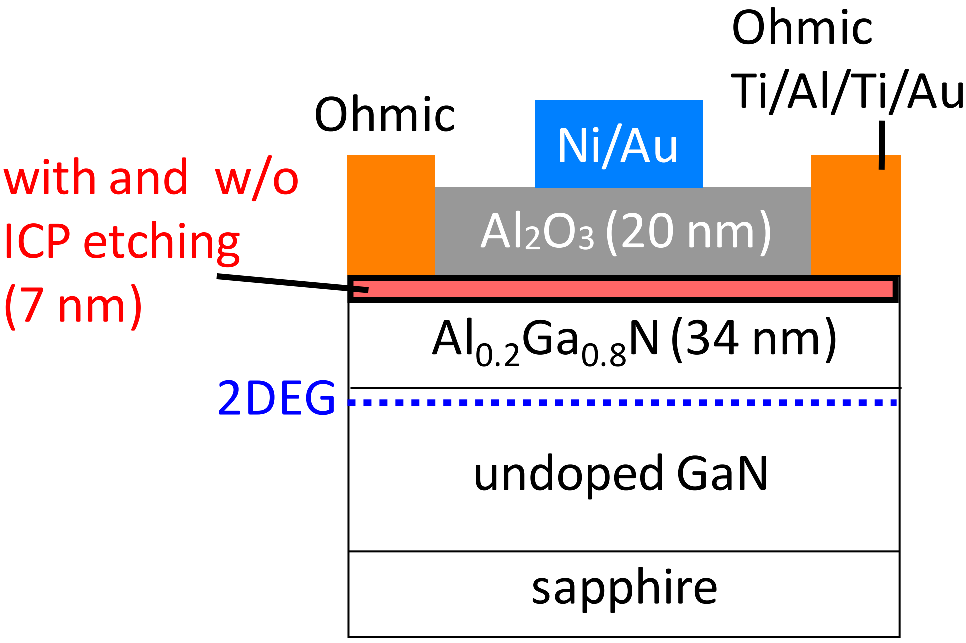
Ohmic
Ti/Al/Ti/Au
Ohmic
Ni/Au
with and w/o
ICP etching
(7 nm)
Al2O3 (20 nm)
Al0.2Ga0.8N (34 nm)
2DEG
undoped GaN
sapphire

Figure 2

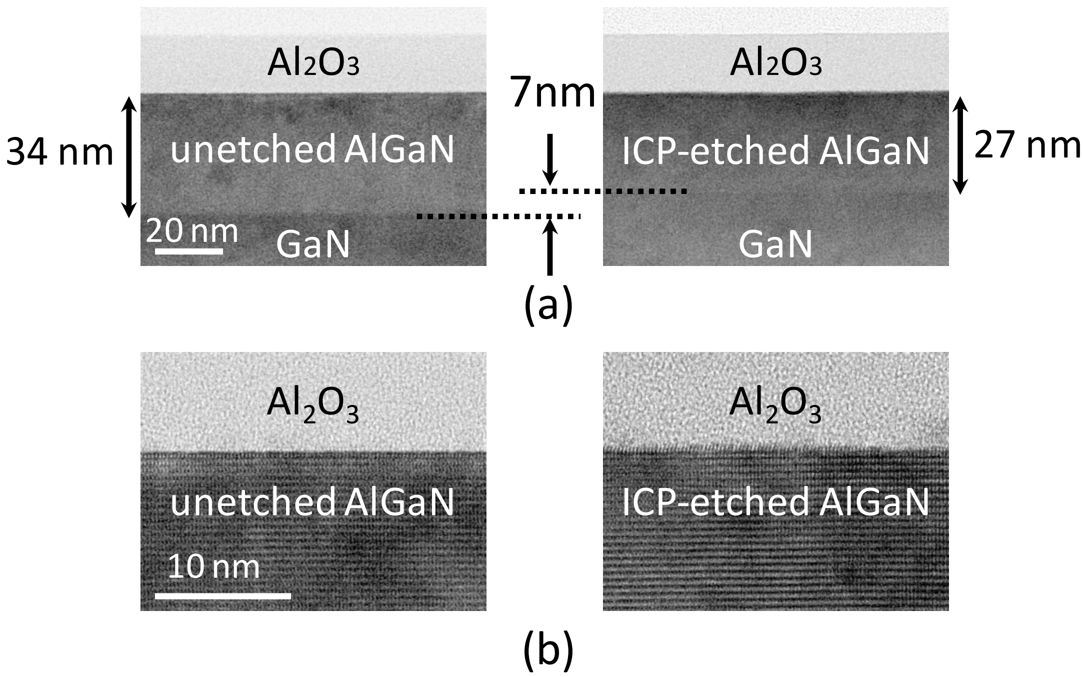

Al2O3
Al2O3
7nm
34 nm
unetched AlGaN
ICP-etched AlGaN
27 nm
20 nm
GaN
GaN
(a)
Al2O3
Al2O3
unetched AlGaN
ICP-etched AlGaN
10 nm
(b)

Figure 3

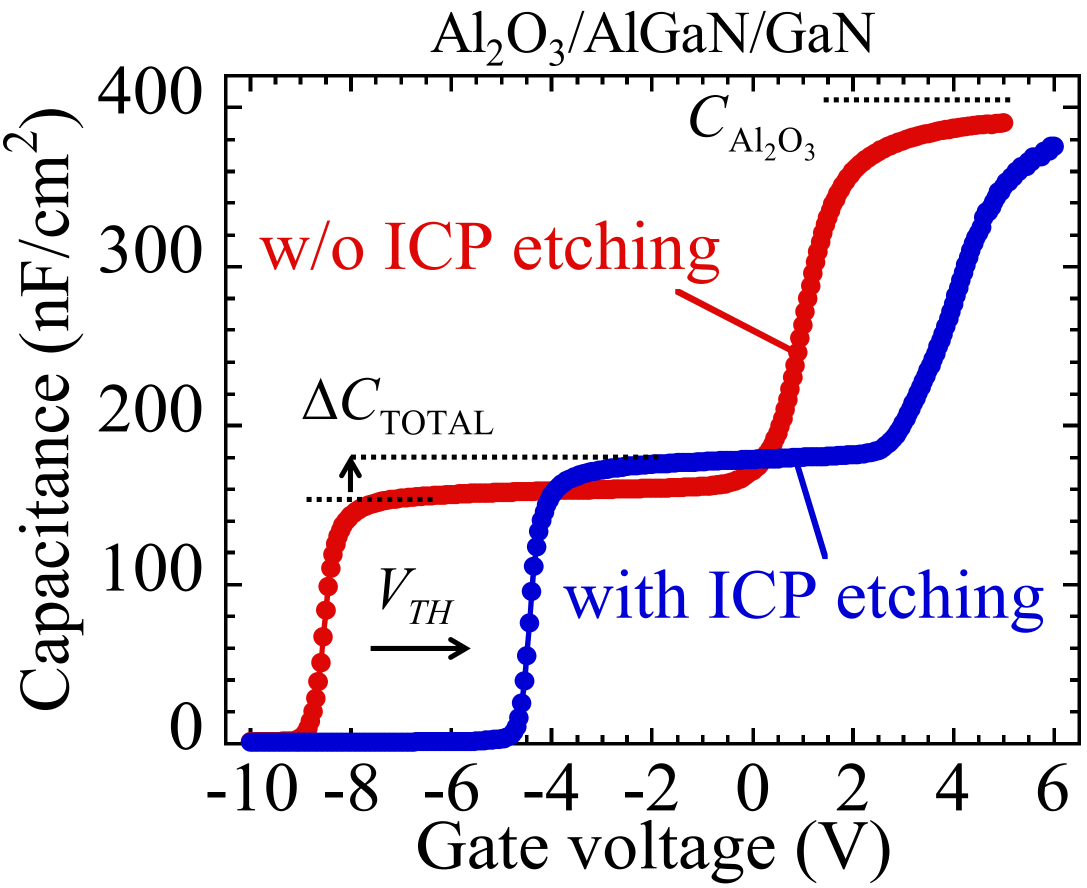

Al2O3/AlGaN/GaN
400
300
200
100
0
Capacitance (nF/cm2)
CAl2O3
w/o ICP etching
ΔCTOTAL
VTH
with ICP etching
-10 -8 -6 -4 -2 0 2 4 6
Gate voltage (V)

Figure 4

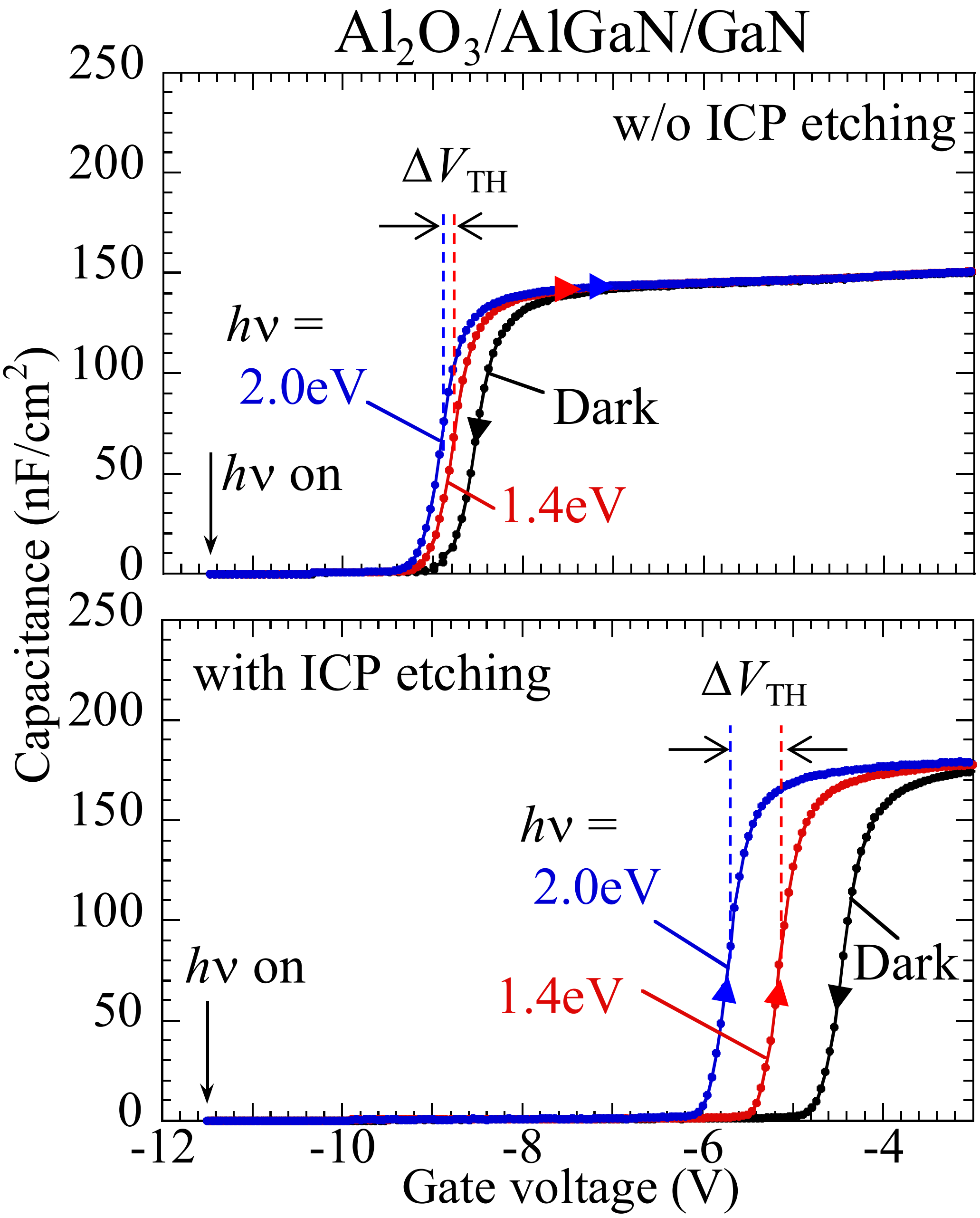

Al2O3/AlGaN/GaN
w/o ICP etching
ΔVTH
hν =
2.0eV
Dark
hν on
1.4eV
with ICP etching
ΔVTH
hν =
2.0eV
Dark
hν on
1.4eV
Capacitance (nF/cm2)
Gate voltage (V)
250
200
150
100
50
0
-12
-10
-8
-6
-4

Figure 5

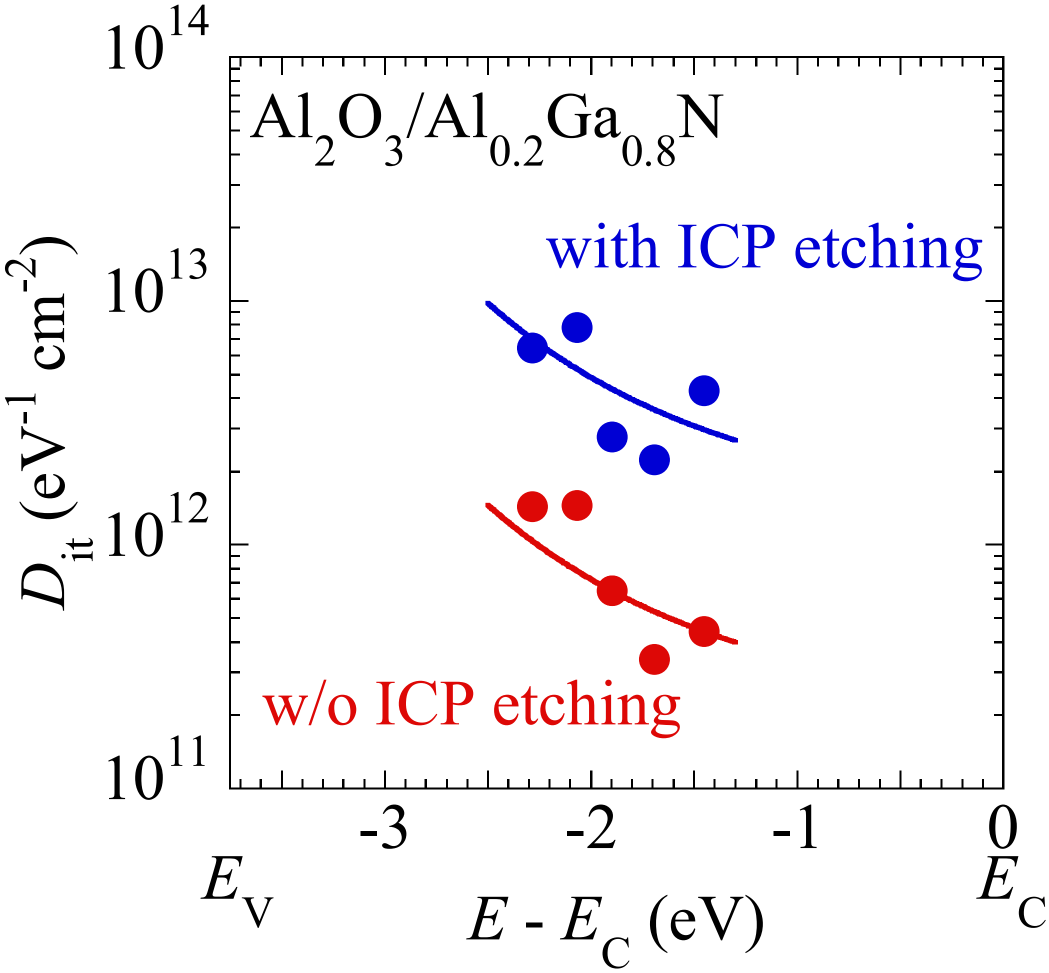

10^14
10^13
10^12
10^11
Al2O3/Al0.2Ga0.8N
with ICP etching
w/o ICP etching
Dit (eV-1 cm-2)
-3
-2
-1
0
EV
E - EC (eV)
EC